ELSEVIER

Polymer 41 (2000) 3683–3692

polymer

Static and dynamic light scattering of maleic acid copolymers

G.C. Chitanu[a,b,*], M. Skouri[c], F. Schosseler[a], J.P. Munch[a], A. Carpov[b], S.J. Candaua[a]

[a]*Laboratoire de Dynamique des Fluides Complexes, UMR 7506, CNRS-Université Louis Pasteur, 4 rue Blaise Pascal, 67070 Strasbourg, France*
[b]*Romanian Academy, "Petru Poni" Institute of Macromolecular Chemistry, Al. Gr. Ghica Voda nr. 41A, 6600 Iasi, Romania*
[c]*Faculté des Sciences, Département de Physique, Université Cadi Ayya, Semlalia, B.P. S15, Marrakech, Morocco*

Received 12 April 1999; received in revised form 15 July 1999; accepted 29 July 1999

Abstract

We study aqueous solutions of maleic acid–vinyl acetate alternating copolymers in a wide range of polymer C and salt C_s concentrations by means of static and dynamic light scattering. Depending on C and C_s, the decay of the autocorrelation function of the scattered electric field is characterized by one or two modes of relaxation. This feature allows one to define the dilute and semi-dilute regimes in a diagram C–C_s. The fast mode of relaxation has the usual behavior reported for polyelectrolyte solutions. The slow mode of relaxation can be linked with the occurrence of chain aggregation. The proposed driving force for the aggregation is the lactonization of the monomers that decreases their solubility in water. Ultimately a phase separation occurs after a time of several weeks that depends on C and C_s. © 2000 Elsevier Science Ltd. All rights reserved.

Keywords: Static and dynamic light scattering; Maleic acid copolymers; Polyelectrolyte solutions

1. Introduction

Maleic acid copolymers are known for their biomedical applications as drugs and as drug or enzyme carriers [1–5]. The polyelectrolyte behavior of alternating maleic acid copolymer in aqueous solution was presented in many reports. Several characteristic properties have been studied the two-step dissociation of carboxylic groups [6–10] and binding of counterions [11–13], pH-induced conformational transitions [14–17], a remarkable behavior of viscosity that exhibits a maximum at the half-neutralization point [10,14,17,18]. These results were obtained from potentiometric, viscometric, conductometric, dilatometric and calorimetric measurements.

Static or dynamic light scattering experiments were much less used to study maleic acid copolymers. A study of a maleic anhydride–ethyl vinyl ether copolymer in anhydride, acidic or Na salt form by means of static light scattering (SLS) and viscometric measurements provided information about molecular weight of the copolymer and its conformation in solution [19]. Dynamic light scattering (DLS) measurements performed on the same copolymer exhibited a conformational transition that had not been observed with other methods [20].

On the contrary, DLS measurements were intensively used in the last years to investigate the interaction between opposite charged polyelectrolytes, particularly between synthetic polyelectrolytes and various proteins [21]. The characterization of polymeric systems for drug or gene controlled delivery was also studied by means of DLS and it seems that this topic is in progress [22,23].

In this paper we report an experimental study of a maleic acid-alt-vinyl acetate copolymer in aqueous solution, without or with low molecular electrolyte, using static and dynamic light scattering techniques. Owing to its chemical structure, this polymer can tolerate high concentrations of added salt even at high polymer concentration allowing an extensive study in a wide range of polymer and salt concentrations.

2. Experimental

2.1. Polymer synthesis

A sample of maleic anhydride (MA)-alt-vinyl acetate (VA) copolymer (I) was synthesized by radical copolymerization of equimolar quantities of MA and VA in benzene, using benzoyl peroxide as initiator [24]. All the substances used were purified by the known methods [25,26]. The

* Corresponding author. National Institute of Bioscience and Human Technology, 1-1 Higashi, Tusukuba, Ibaraki 305, Japan. Tel.: +40-32-140413, extn: 34; fax: +40-32-211-299.
E-mail address: chita@ichpp.tuiasi.ro (G.C. Chitanu).

PII: S0032-3861(99)00560-1

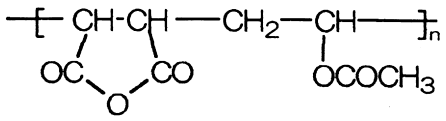

Scheme 1.

chemical composition of I was assessed by conductometric titration in 1:1 (vol) acetone–water mixture with 0.1 N aqueous NaOH [27], using a radiometer AB Copenhagen conductometer type CDM 2d and a CDC 114 cell. The acid number was 0.439 g NaOH/g, corresponding to a 1:1 (moles) ratio between MA and VA units. The ^{1}H NMR spectrum was recorded with a Brucker AC 300 MHz spectrometer, using deuterated acetone as solvent and its signal at $d = 2.05$ ppm as the internal standard. The IR spectrum was recorded with a Perkin–Elmer 577 spectrophotometer in KBr pellet. Both spectra were in agreement with a rather alternating distribution of monomers along the polymer chain [28,29], according to the chemical formula presented in Scheme 1 which depicts the chemical structure of MA-alt-VA copolymer.

The molecular weight of I estimated from viscometric measurements [30] was 10^5 Da, corresponding to a polymerization degree $n \sim 540$.

2.2. Preparation of samples

The solvent used was deionized water purified by a Milli-Q purification system, with or without a low molecular electrolyte (LWE). The LWE were pro analysi NaCl or HCl (Merck). Before the preparation of polyelectrolyte solutions the solvent was filtered through Millipore GS 0.22 μm pore size filter. To clear it from the air bubbles the NaCl or HCl solution was prepared at least 1 day before diluting the samples.

The samples were prepared from stock solutions with concentration 1–2 g/dl, obtained by polymer dissolution in water, at room temperature, during 24 h. Other authors have mentioned longer dissolving periods of time [31] and heating of solutions, but we have avoided such conditions because of the chemical structure of our copolymer. In water the anhydride rings undergo hydrolysis and a MA–VA copolymer (II) is obtained with the chemical structure of maleic acid-alt-vinyl acetate copolymer presented in Scheme 2.

It was checked by conductometric titration and IR spectra that this sample preparation allows a complete reaction of anhydride units. A sample of II prepared according to this method was spray-dried and examined by conductometric

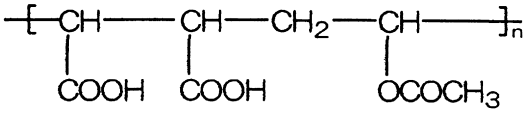

Scheme 2.

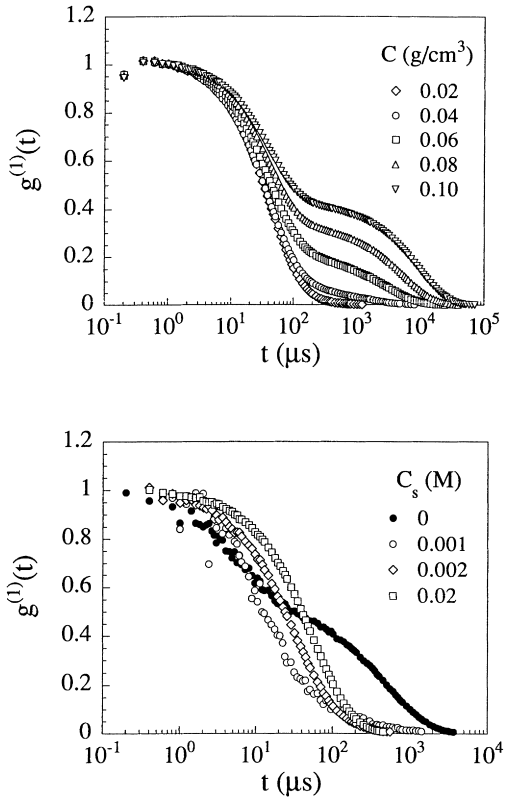

Fig. 1. Effect of polymer and salt concentrations on the shape of the correlation functions: (top) at $C_{NaCl} = 1$ M, varying C. Below $C = 2 \times 10^{-2}$ g/cm^3 the decay can be considered as monomodal; (bottom) at $C = 0.125 \times 10^{-2}$ g/cm^3, varying C_S. For $C_{NaCl} \geq 2 \times 10^{-3}$ M, the decay can be considered as monomodal.

titration and IR spectra. The acid number was 0.384 g NaOH/g corresponding to a 99.7% conversion. In the IR spectra the bands at 1850 and 1780 cm^{-1} ascribed to anhydride cycles disappeared.

The stock solutions were diluted with water or NaCl or HCl stock solution and they were allowed to homogenize 12–24 h at room temperature. The light scattering measurements were performed after 2–4 h of centrifugation. Our experiments were carried out at a polymer concentration C between 5×10^{-4} g/ml (2.7×10^{-3} monomol/l) and 10^{-1} g/ml (5.4×10^{-1} monomol/l).

2.3. Light scattering measurements

The optical source of the light-scattering apparatus was a Spectra-Physics argon ion laser operating at $\lambda = 4880$ Å. An Amtec Goniometer allowed to vary the scattering angle θ between 20 and 140°. This allows scattering wavevectors q in the range of $6 \times 10^{-4} \leq q$ (Å^{-1}) $\leq 3 \times 10^{-3}$. In the dynamic light scattering (DLS) experiments, the time dependent correlation function of the scattered intensity was obtained by using a 64-channels digital correlator Brookhaven BI 2030 or a correlator ALV 5000 with 256 channels. This latter was used to record the correlation functions presenting two distinct decay rates. The samples were

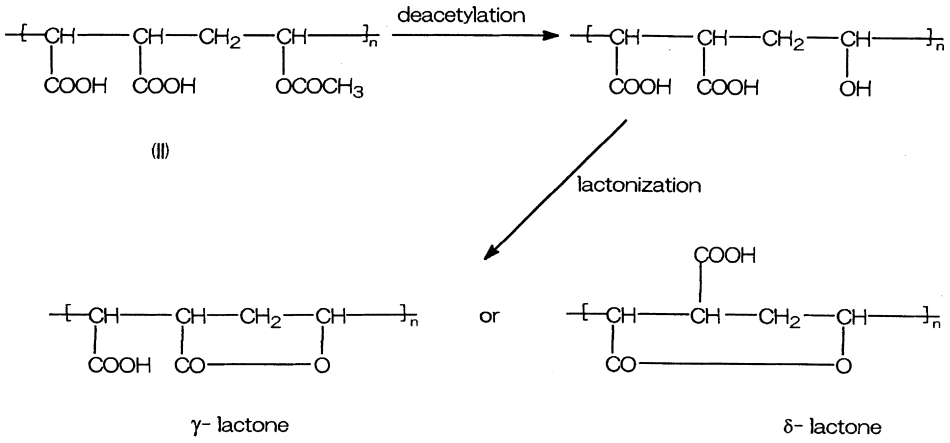

Scheme 3.

thermostated during the measurements at 20 ± 0.1°C. As low molecular electrolytes, NaCl with a concentration, C_s between 10^{-3} and 2 M or HCl with a concentration, C_a between 2×10^{-2} and 1 M were used.

Static scattering intensities $I(q, C)$ were normalized by the intensity I_{tol} scattered from a toluene standard. In the dilute regime of polymer concentration, linear fitting of $I_{tol}/I(q, C)$ vs. q^2 plots yielded values for the zero-angle scattering intensity I_0 (in units of toluene scattering intensity) and for an apparent radius of gyration. The latter was found in most cases to be too small to be considered reliable.

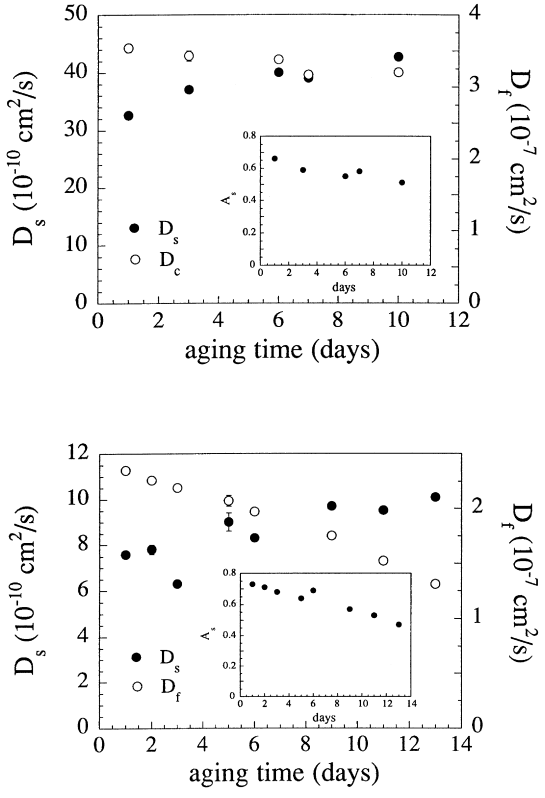

Fig. 2. Evolution with aging time of the apparent diffusion coefficients measured at $q = 90°$. The inserts show the time evolution of the amplitude of the slow mode: (top) $C = 4 \times 10^{-2}$ g/cm^3, $C_S = 0.2$ M; (bottom) $C = 10^{-1}$ g/cm^3, $C_S = 2\ M$.

Dynamic light scattering experiments provided the normalized time correlation function $g^{(2)}(q, t)$ of the scattered intensity (ICF) defined as:

$$g^{(2)}(q,t) = \frac{\langle I(q,0)I(q,t)\rangle}{\langle I(q,0)\rangle^2} \tag{1}$$

where $I(q, t)$ is the scattered intensity at time t. If the scattered field is assumed to have Gaussian statistics, the normalized intensity autocorrelation function $g^{(2)}(q, t)$ is directly related to the normalized electric field autocorrelation function $g^{(1)}(q, t)$ through the Siegert relation:

$$g^{(2)}(q,t) = 1 + A|g^{(1)}(q,t)|^2 \tag{2}$$

where A is an equipment-dependent amplitude factor. Depending on the polymer and salt concentrations, $g^{(1)}(q, t)$ was characterized by a single mode of relaxation or by two more or less separated modes of relaxation (Fig. 1). In a few cases, there was some evidence for a third relaxation mode.

The monomodal correlation functions were analyzed by a cumulant expansion fit to calculate the average decay rate $\langle \Gamma \rangle$ and the variance. The correlation functions $g^{(1)}(t)$ showing two modes of relaxation were fitted using the CONTIN program [32]. The areas A_i of the distribution peaks were calculated as well as the corresponding average decay rates Γ_i or the apparent diffusion coefficients $D_i \equiv \Gamma_i/q^2$. They were labeled as $i =$ f and s for the fast and slow mode of relaxation, respectively. Note that we have $A_f + A_s = 1$ when only two modes are present.

For the polymer solutions in pure water or at low salt content ($C_s \leq 10^{-3}$ M), the DLS experiments were repeated until the scattering intensity remained stable during an experiment. Generally, the values presented are averaged from several experiments.

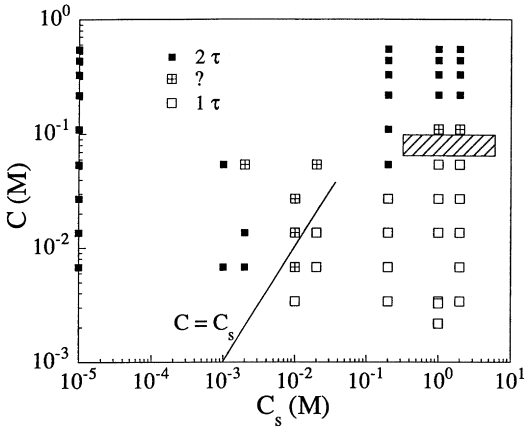

Fig. 3. C–C_S diagram: the open and full squares correspond to a monomodal or bimodal decay of $g^{(1)}(t)$, respectively. Crossed squares represent cases where the distinction is difficult and, in some instances, the CONTIN analysis yields three decay modes (see in the text). The overlap concentration C^* was estimated using the R_h measured by DLS in dilute regime and is shown as the dashed area. The boundary line corresponds to $C = C_S$.

2.4. Time stability of solutions

The chemical structure of MA–VA copolymer allows some secondary reactions as deacetylation, esterification, lactonization [33]. In acid solution, at higher temperature it can be observed a deacetylation of about 60% and a lactonization [34], according to Scheme 3 which shows the chemical reactions of MA-alt-VA copolymer by decreasing its solubility.

The lactone rings strongly lower the water solubility of the copolymer. To avoid these undesired reactions in the industrial production of MA–VA copolymer the synthesis conditions such as temperature, pressure, and time must be carefully checked [35]. Taking into account these phenomena we have performed DLS measurements for samples with different polymer and salt concentrations at times of 1–14 days from sample preparation. The ICFs were obtained at $\theta = 90°$ and the apparent diffusion coefficients of fast and slow modes were evaluated. In Fig. 2 are presented some of the results concerning the time evolution of DLS parameters at various C and C_s.

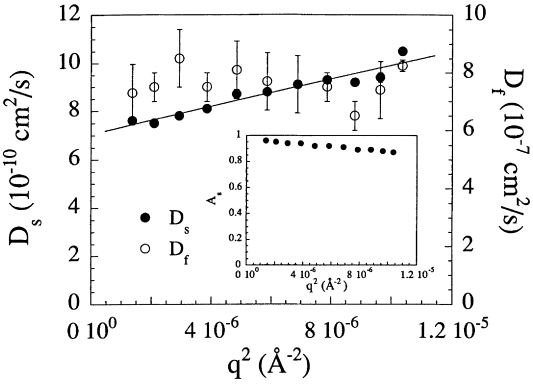

Fig. 4. Dependence of apparent diffusion coefficients D_f and D_s on the squared wavevector ($C = 8 \times 10^{-2}$ g/cm^3, $C_S = 0$). In the insert is presented the q^2 dependence of the amplitude of the slow mode.

As a general trend, D_s increases and D_f decreases with aging while the slow relaxation becomes less important, i.e. its amplitude decreases. After a few months, the samples are phase-separated with the formation of a gel-like opaque phase at the bottom of the cell. The time evolution is more pronounced for large values of C and C_s. It could be explained by the secondary reactions mentioned above and also by a "salting out" effect already known for polyelectrolyte solutions [36]. Some other polylectrolytes as poly(adenylic acid) or linear poly(ethyleneimine) were reported to present a similar behavior [37,38], whereas sodium poly(styrenesulfonate) solutions provided quite constant ICF's [38–43]. All these observations suggested us to avoid the sample preparation several days before LS experiments. Generally a set of measurements in which was checked the influence of a parameter like C, C_s, q, was performed on the same or next day.

3. Results and discussion

3.1. General features of the static and dynamic light scattering results and diagram C–C_s

Depending on the salt concentration and the polymer concentration, $g^{(1)}(t)$ is monomodal or bimodal. In a few cases it is more complex and the CONTIN program gives three components. Examples are given in Fig. 1. In the top portion of the figure, correlation functions obtained for systems with the same salt content $C_s = 1$ M and various polymer concentrations show that, at low polymer concentration ($C \leq 2 \times 10^{-2}$g/cm^3), the decay of $g^{(1)}(t)$ is governed by a single mode of relaxation whereas, at a higher concentration, a slow mode shows up whose amplitude increases with C. In the bottom portion of Fig. 1, the correlation functions obtained at fixed polymer concentration ($C = 0.125$ g/cm^3) show two modes of relaxation at low salt content. Above $C_s = 2 \times 10^{-3}$M, the distribution of relaxation rates can be considered as monomodal.

The ensemble of observations concerning the shape of $g^{(1)}(t)$ can be summarized diagramatically C–C_s (Fig. 3). A single exponential decay of $g^{(1)}(t)$ is observed at high salt and low polymer concentrations. In the rest of the diagram one observes essentially two modes of relaxation.

The q dependences of the slow and fast relaxation modes give more information on the structural properties of the systems investigated. We have not analyzed in detail all systems shown in Fig. 3 but the following general features can be drawn out.

In the case where one observes a monomodal correlation function, the relaxation rate varies as q^2, thus indicating a diffusive process characterized by a diffusion coefficient D. As this region corresponds to dilute solutions with screened electrostatic interactions, one is entitled to calculate from D

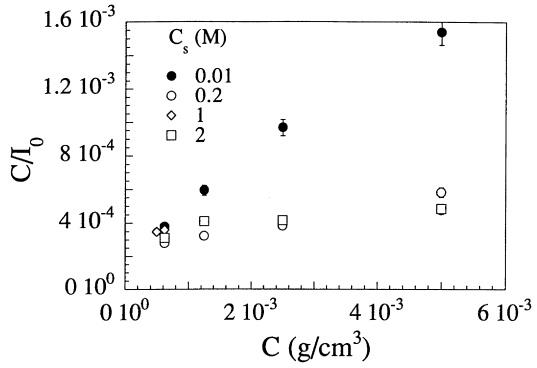

Fig. 5. Dependence of ratio C/I_0 on polymer concentration for different concentrations of NaCl.

the value of an hydrodynamic radius through the Stokes–Einstein relationship.

In the case where the decay of the correlation function exhibits two modes of relaxation, one obtains again a q^2 dependence for the fast relaxation rate Γ_f whereas the characteristic rate of the slow mode generally obeys an equation of the form:

$$\frac{\Gamma_s}{q^2} = D_s(0)(1 + cq^2) \tag{3}$$

where c is a positive constant.

In Fig. 4 is given an example of this behavior corresponding to a salt free solution with $C = 0.08$ g/cm^3. The insert of this figure shows the variation with q^2 of the amplitude of the slow mode $A_s(q)$. Usually this variation can be well described by a law of the form:

$$A_s(q) = A_s(0)(1 - c'q^2) \tag{4}$$

where c' is a positive constant.

We will come back later on the behavior of the systems with two modes of relaxation and focus first on the simplest cases where only one mode of relaxation is present in $g^{(1)}(t)$.

3.2. Dilute regime with screened electrostatic interactions

This regime corresponds to the points located in the lower right corner of the diagram in Fig. 3. The polymer concentration ranges from 6.25×10^{-4} to 10^{-2} g/cm^3 and the salt concentrations from 10^{-2} to 2 M. In this domain of salt content, one can expect the electrostatic interactions to be screened to a large extent and because the polymer concentration is small, we are likely to be in the dilute regime as already stated above. The experimental results are in agreement with this expectation.

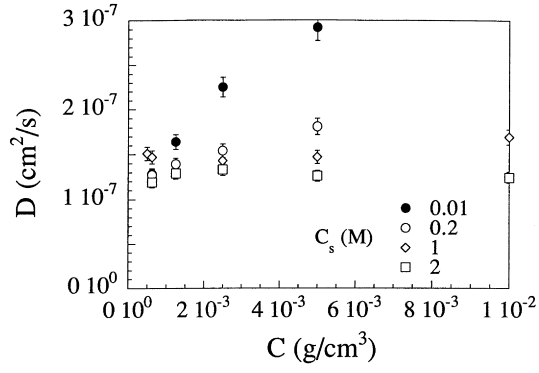

Fig. 6. Dependence of average diffusion coefficient on polymer concentration in the dilute regime for different salt concentrations.

Static light scattering intensity shows a very weak dependence on q. The experimental accuracy does not allow us to determine from these experiments the radius of gyration, which would indicate for the latter values below about 260 Å. Fig. 5 shows the concentration dependences of C/I_0 for different salt contents. Within the experimental accuracy, the variation of C/I_0 with C can be described by straight lines extrapolating to the same origin. This origin is proportional to the inverse of the weight average molecular weight. The slope of C/I_0 vs. C, which is a measure of the second virial coefficient, is a decreasing function of the salt concentration. This effect is characteristic of polyelectrolyte solutions and can be attributed to the screening of the electrostatic interactions by the added salt. At high salt concentrations the interactions are dominated by the excluded volume of the neutral polymer. It can be seen in Fig. 5 that in the high salt content regime ($C_s \geq 1$ M), the slope of C/I_0 vs. C is still positive.

The results of static light scattering are confirmed by the dynamic light scattering measurements. In the investigated C–C_s region, $g^{(1)}(t)$ can be analyzed by the cumulant method, the experimental variance being less than 0.2. Fig. 6 shows the variation of the diffusion coefficient D as a function of C for different salt contents. These variations can be described by straight lines whose slope decreases smoothly upon increasing the salt content. This behavior as well as the zero slope at high salt content can be compared with the effect of added salt on the second virial coefficient (Fig. 5). The differences illustrate the intricate effects of thermodynamic and hydrodynamic interactions that govern the variation of D with polymer concentration. The straight lines representative of $D(C)$ extrapolate at $C = 0$ to the same ordinate within the experimental accuracy $D_0 = 1.2 \times 10^{-7}$ cm^2 s^{-1}. From the Stokes–Einstein relation one obtains for the hydrodynamic radius $R_H = 176 \pm 20$ Å, in agreement with the weak dependence of the static scattering intensity on the scattering vector.

One is tempted to infer from these results that, at high salt concentration, the apparition of a second mode of relaxation with the increasing polymer concentration corresponds to the transition between the dilute and the semidilute regimes of polymer concentration. Indeed an estimation of the overlap concentration C^* from the above measured hydrodynamic radius is shown as the dashed area in Fig. 3 and is in agreement with this picture.

We have also performed light scattering measurements on copolymer solutions containing from 10^{-2} to 1 M of hydrochloric acid (HCl). The addition of HCl shifts the

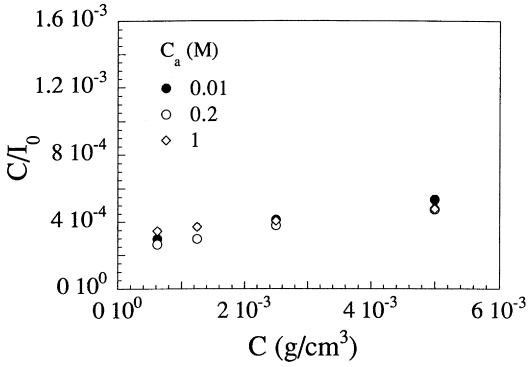

Fig. 7. Dependence of ratio C/I_0 on polymer concentration for different concentrations of HCl. To facilitate the comparison with Fig. 5, the axis scales have been set the same.

acido-basic equilibrium so that the dissociation of carboxylic groups is reduced. Figs. 7 and 8 illustrate the effect of the addition of HCl on the concentration dependence of C/I_0 and D. The observed behavior is strikingly different from that obtained on the addition of NaCl. A concentration of the added HCl as small as 10^{-2} M is enough to suppress the effect of the electrostatic interactions as inferred from the C/I_0 vs. C curves. Some differences in the extrapolated values of C/I_0 and D in Figs. 5–8 are within the experimental accuracy, but small effects of the nature of the LWE on the hydrodynamic radius (for $D(C)$) and on the refractive index increment (for $C/I_0(C)$) cannot be excluded.

The effects of the added HCl can be understood in terms of displacement of the dissociation equilibrium as for poly(acrylic acid) or poly(methacrylic acid). The dissociation of the carboxylic groups in the copolymers of maleic acid is a two-step process, because of the strong electrostatic interactions between neighbor groups, with $pK_1 \sim 3$–4 and $pK_2 \sim 7$–10 [44]. The difference between these two values result mainly from the inductive effects of the adjacent carboxylic groups. The presence of neighboring dipoles favors the ionization of carboxylic groups. Once the first carboxylic group dissociated, the dissociation of the second one is unfavored by the repulsive electrostatic effect of the

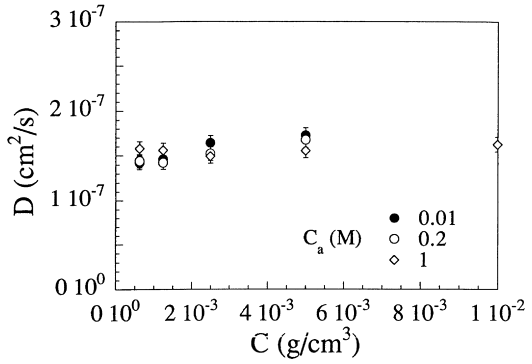

Fig. 8. Dependence of average diffusion coefficient on polymer concentration in the dilute regime for different acid concentrations. To facilitate the comparison with Fig. 6, the axis scales have been set the same.

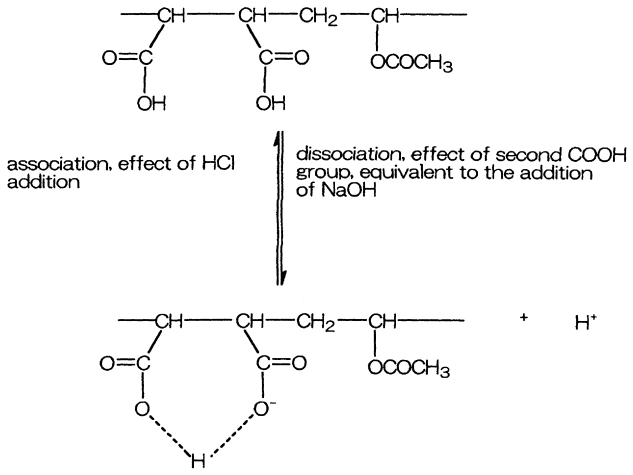

Scheme 4.

charge formed. The monocarboxylate ion is stabilized by the chelation of the proton of the second carboxylic group according to Scheme 4 which shows the dissociation equilibrium in aqueous solution of MA-alt-VA copolymer.

Light scattering results can be related to the fact that in the absence of salt (pH ~ 2–3) only one carboxylic group of the copolymer is dissociated. Under addition of a small amount of HCl, the equilibrium is shifted towards the top in Scheme 4, the copolymer becomes quasi-neutral and the interactions are only due to the polymer excluded volume.

3.4. Semidilute regime

We consider now the systems located on the left-hand side and above the boundary lines drawn in the diagram in Fig. 3. They are all characterized by a bimodal autocorrelation function of the scattered light. Fig. 9 shows the amplitude of the slow mode measured at $\theta = 90°$ as a function of polymer concentration for different salt contents. In the absence of added salt, the slow mode is predominant in the whole range of polymer concentration investigated and A_s keeps a constant value of about 0.8 irrespective of the polymer concentration. On the contrary, in the presence of salt, A_s is a monotonously increasing function of the

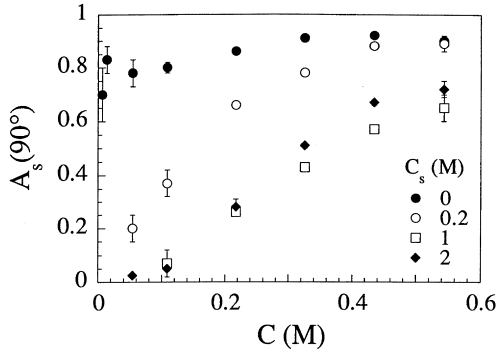

Fig. 9. Polymer concentration dependence of the amplitude of the slow mode ($q = 90°$) for different salt contents.

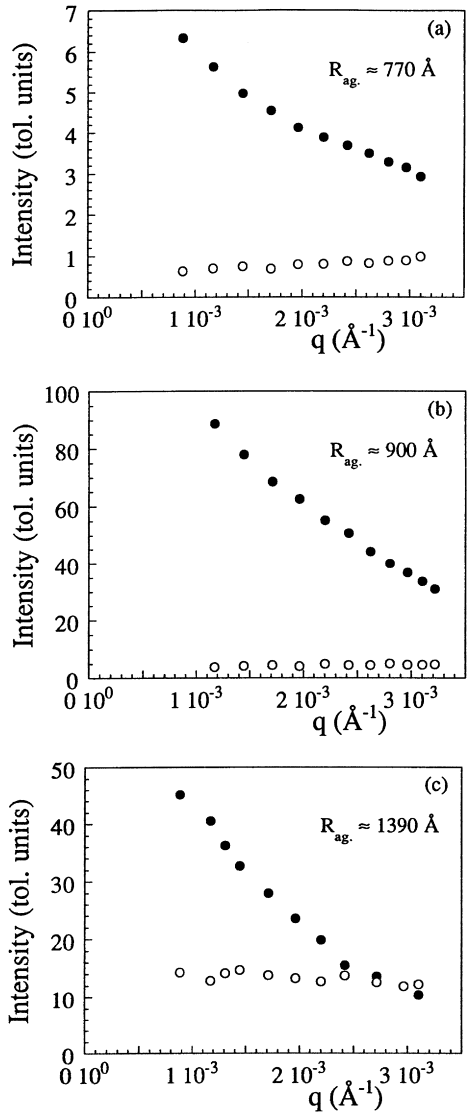

Fig. 10. Splitting of the total scattering intensity into the contributions from the intensities associated to the fast (open circles) and slow (full circles) components for different experimental conditions: (a) $C = 2 \times 10^{-2}$ g/cm^3, $C_S = 0$; (b) $C = 8 \times 10^{-2}$ g/cm^3, $C_S = 0$; (c) $C = 10^{-1}$ g/cm^3, $C_S = 1$ M. The indicated values for the apparent radius of gyration R_{ag} are obtained from the q^2 dependence of $I/I_S(q)$ (see text).

polymer concentration. Its extrapolation to $C = 0$ coincides with the shaded area in Fig. 3. For a fixed polymer concentration, e.g. $C \approx 0.5$ M, A_s seems to be a non-monotonous function of the salt concentration but this appearance could be a mere consequence of different angular dependences for A_s as a function of salt content (see for example Fig. 4). No time was available to explore that feature in detail.

The q dependence of both Γ_s and A_s is consistent with the scattering behavior of polydisperse aggregates in dilute solution [45] and can be possibly considered as a signature of the presence of clusters of chains. Thus an explanation for the slow mode observed in our solutions would be the occurrence of aggregation. Following this idea, we can then assume that the electric field scattered from the solution can be split into two contributions arising from the aggregates and from the remaining solution. Standard derivation then shows that this distinction allows one to split the total static scattering intensity $I(q)$ (in toluene scattering units) into the contribution of aggregates and of the remaining solution as [46–50]:

$$I_s(q) = A_s(q)I(q) \tag{5}$$

$$I_f(q) = A_f(q)I(q)$$

Fig. 10 illustrates the results of this procedure for some of our samples and it is clearly apparent that the angular dependence of the total scattering intensity is attributed to the intensity $I_s(q)$ scattered from the aggregates while the intensity associated with the fast fluctuations of concentration is q independent within the experimental accuracy for the three examples shown in Fig. 10. Standard linear analysis of $I/I_s(q)$ vs. q^2 plots yields apparent radii of gyration $R_{ag.} \sim 10^3$ Å (see Fig. 10).

Fig. 11 displays the variation with polymer concentration ($C_s = 1$ M) of the total intensity I_{90} scattered at $\theta = 90°$, the total scattering intensity I_0 extrapolated at zero angle, the intensity, $I_{f,90}$ associated with the fast mode ($\theta = 90°$) and the corresponding value $I_{f,0}$ extrapolated at zero angle for one polymer concentration ($C = 0.10$ g/cm^3). For the latter value to be calculated, it is necessary to perform DLS experiments in the whole range of scattering vectors to obtain $A_s(q \to 0)$. These time consuming measurements could not be done for all the samples. One example is given here to show the trends. In the whole range of polymer concentration, the total scattering intensities I_0 and I_{90} are increasing functions of the polymer concentration. This behavior contrasts with that of solutions of neutral polymers for which the zero angle scattering intensity goes through a maximum in the vicinity of C^* and then decreases as a power law of concentration with an exponent -0.31 (good solvent) or -1 (theta solvent). On the contrary, the latter behavior is observed for $I_{f,90}$ and the $I_{f,0}$ measured for $C = 0.10$ g/cm^3 shows that $I_{f,0}$ would exhibit the same trend if it would be measured in the whole range of concentration. Although the exponents measured here at $\theta = 90°$ are in the good range (-0.32 for $C_s = 0.2$ M and -0.61 for $C_s = 2$ M), the correction for the angular variation is likely to affect slightly these values. Thus the intensity associated to the fast relaxation behaves with polymer concentration as in regular semidilute solutions of neutral polymers. The maximum is located around $C = 0.02$ g/cm^3 which is again consistent with our estimation for the overlap concentration C^* in Fig. 3. This means that the increase of the total intensity with polymer concentration above C^* is because of the intensity associated with the slow mode of relaxation which is in agreement with the hypothesis that aggregates are present at these concentrations.

A similar analysis can be made with the same parameters measured at $C_s = 0$ (Fig. 12). In the absence of salt, it is remarkable that we get $I_{f,90} \infty C$, in full agreement with the

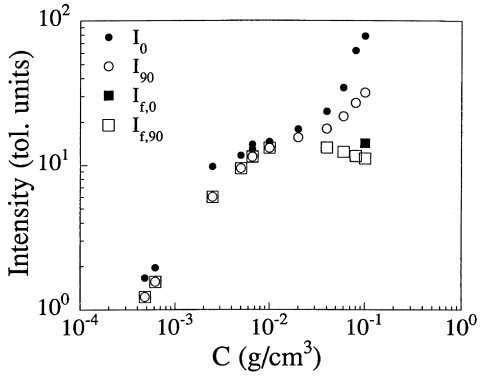

Fig. 11. Variation with polymer concentration of the total scattering intensity and of the intensity I_f associated with the fast process of relaxation ($C_S = 1$ M). Subscripts 0 and 90 refer to values extrapolated at zero scattering angle and measured at $\theta = 90°$, respectively.

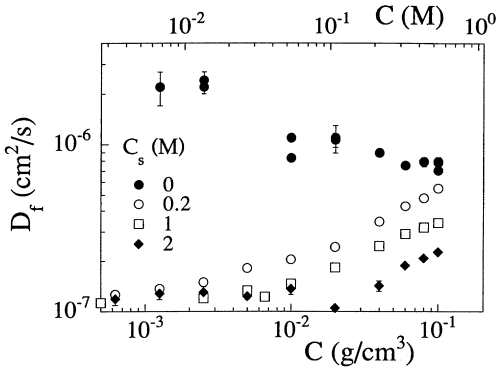

Fig. 13. Variation of the fast diffusion coefficient with polymer concentration for different salt contents.

expected variation for the scattering intensity of a polyelectrolyte solution where the osmotic compressibility is governed by the entropy of the counterions [51]. Again it would be necessary to perform a full analysis and get $I_{f,0}$ as a function of polymer concentration to bring a definitive conclusion but the trends are clearly present.

Thus, from the above results, it seems justified to split the total scattering intensity as the sum of the contributions arising from aggregates and from a regular semi-dilute solution. For the latter contribution, depending on the salt concentration, the behavior is characteristic of a polyelectrolyte solution or of a neutral solution (screened polyectrolyte regime). We can now turn to the behavior of the apparent diffusion coefficients associated to the two modes of relaxation.

In Fig. 13 is reported the variation of the fast diffusion coefficient with the polymer concentration for different salt contents. In salt free solutions, there seems to be a trend for a small decrease of D_f by a factor about 3 when the concentration is increased in a two-decades range. However, the values measured at the lowest polymer concentrations are obtained under very difficult experimental conditions (low

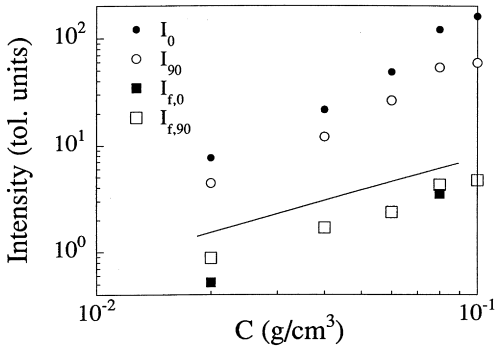

Fig. 12. Variation with polymer concentration of the total scattering intensity and of the intensity I_f associated with the fast process of relaxation ($C_S = 0$). Subscripts 0 and 90 refer to values extrapolated at zero scattering angle and measured at $\theta = 90°$, respectively. The straight line corresponds to a slope unity (see text for details).

scattering intensity, large contribution of the slow mode) and should be considered with caution. In fact, if we discard them, we would better conclude that D_f is rather insensitive to polymer concentration, in agreement with recent works on salt-free polyelectrolyte solutions in this polymer concentration range [39,42,43,52].

In the presence of salt, again a classical behavior for polyelectrolyte solutions [38,40,41] is observed, namely an increase of D_f with polymer concentration, which is in qualitative agreement with the scaling approach [53]. However, for a given polymer concentration, the diffusion coefficient decreases for increasing salt content and previous studies [38,40,41] have shown that this effect cannot be described correctly by this theory. Although some non-trivial effects of salt addition on the thermodynamic quality of the solvent or on the frictional effects have been invoked to explain this discrepancy [38,40,41], more recent works have also shown that the variation of the electrostatic persistence length with ionic strength might be involved [54–56].

Turning now to the slow relaxation rate, as it is generally q dependent according to Eq. (3), one can determine a diffusion coefficient $D_s(0)$ [45], the q dependence of $D_s(q)$ being associated with the large size of the aggregates. The constant in Eq. (3) is proportional to the squared radius of gyration of the aggregates with the proportionality constant varying between 0.1 and 0.2 depending on the shape, conformation and polydispersity of the aggregates [45]. Taking the average value 0.15 for this constant, the deduced radii of gyration are a factor of about 2 smaller than those measured from the q^2 dependence of $I/I_s(q)$ (see above). This fair agreement for values obtained independently thus confirm that the apparent radii of gyration are in the range 500–1000 Å in these samples. On the contrary, using the picture of aggregates diffusing in the semi-dilute solution, we can deduce an apparent hydrodynamic radius $R_{h,ag}$ from $D_s(0)$ by using the Stokes–Einstein relation. If the viscosity of the solvent is used for that calculation, then the ratio $R_{h,ag.}/R_{ag}$. Varies from about 6 ($C = 0.02$ g/cm^3, $C_s = 0$) to about 34 ($C = 0.08$ g/cm^3, $C_s = 0$ M).

This discrepancy was already noted in Refs. [42,43] and

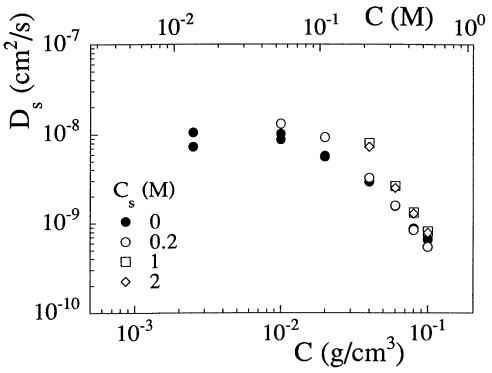

Fig. 14. Variation of the slow diffusion coefficient with polymer concentration for different salt contents (values measured for $\theta = 90°$).

was attributed to the fact that, for aggregates such that the condition $qR_{ag.} \ll 1$ is no longer fulfilled, the apparent diffusion coefficient does no longer reflect the translational diffusion alone but the internal dynamics as well. However, as pointed out by other authors [42,43], the origin of the contrast of the clusters by comparison with the surrounding solution is not clear. If it is a concentration difference, then we have no reason to think in terms of a two-densities model, with well-defined boundaries. Instead, the aggregates would more likely consist of a core, with higher density than the surrounding solution, and a corona, with density comparable or smaller than the surrounding solution. In this picture, the contribution of the static intensity $I_s(q)$ or the q dependence of $D_s(q)$ would come from the cores while, for the dynamics, the influence of the corona would slow down the motion of the aggregates and decrease the value of $D_s(0)$, in agreement with the experimental behavior. This effect could be rather important if the aggregates contained multiple cores.

On the contrary, more recently, it was suggested [50] that, for very large domains ($qR_{ag.} \gg 1$) in a neutral semi-dilute solution (characteristic length ξ), the relaxation of concentration fluctuations with wave vector q such that $q\xi \gg 1$ should involve a viscosity higher than that of the solvent because it occurs through the collective motion of many blobs. However, this idea does not seem to hold true in the NaPSS solutions investigated by Sedlak and Amis [42] as they report a weak dependence of D_s with polymer concentration, i.e. $D_s \sim C^{-x}$ with $x \approx 0.4$, for a comparable degree of polymerization ($n \approx 540$). Nevertheless, in the present system, we obtain a much more pronounced decrease of D_s (Fig. 14) with apparent exponents (determined for $C > 10^{-2}$g/cm^3) ranging between 1.4 (no added salt) and 2.5 ($C_s \geq 1$ M).

For the comparison, Dobrynin et al. [57] calculated the concentration dependence of the viscosity in polyelectrolyte solutions and, in the semi-dilute entangled regime, they predict $\eta \sim C^{3/2}$ in the absence of salt and $\eta \sim C^{15/4}$ in the high-salt regime. In the semi-dilute non-entangled regime, where the overlap of the chains is not large enough to form entanglements, the variations are weaker, i.e. $\eta \sim C^{1/2}$ with no added salt and $\eta \sim C^{5/4}$ with excess of salt. Thus, if only the viscosity of the solution was responsible for the variation of D_S with polymer concentration, our data would be consistent with the prediction of the semi-dilute entangled regime in the absence of salt while the data obtained at high salt concentration would correspond to some crossover between the entangled and the unentangled regimes. However, we have to keep in mind that the size of the diffusing aggregates is very likely dependent on the polymer concentration [42,43] and that this point could be settled down only through a thorough study of the angular dependence of $D_s(q)$ for all the experimental conditions. In fact, the values reported in Fig. 14 have been measured for a fixed scattering angle ($\theta = 90°$) and no definitive conclusions can be reached.

3.5. Final remarks

As mentioned at the beginning of this paper, our solutions present a significant evolution with time and ultimately a phase separation takes place after a few months. A possible explanation for this evolution is the progressive aggregation of the polymers as the lactonization takes place as depicted in Scheme 3. Thus our solutions cannot be considered as model polyelectrolyte solutions, where the electrostatic interactions are dominant, and the driving force for the aggregation is probably different than in NaPSS solutions, although hydrophobic forces have been shown to play a significant role in the latter [58]. Therefore our results should not be used in the heated debate about the origin of the slow mode in polyelectrolyte solutions [59].

We can mention that we tried to filter some of the salt-free solutions and obtained qualitatively different behavior about the amplitude of the slow mode, which was then observed to decrease with decreasing polymer concentration. Presumably this behavior is masked in unfiltered solutions by the predominant aggregation that ultimately leads to phase separation. This experimental procedure was not pursued further because it did not correspond to the original scope of this paper, which was the characterization of the MA–VA copolymer solutions. Afterwards, it might be necessary to use filtration in order to investigate the formation of intermacromolecular complexes upon addition of drugs or other additives since, without filtration, this phenomenon might be masked by the aggregation evidenced in the present paper.

4. Conclusion

The set of results reported here is the first attempt to investigate aqueous solutions of maleic acid copolymers by means of static and dynamic light scattering in a wide range of polymer and salt concentration. According to the shape of the autocorrelation functions obtained by dynamic light scattering a diagram was established in which monomodal autocorrelation functions are located at low C and high C_S while bimodal autocorrelation functions are found

at high C whatever is C_S, in general agreement with existing data for other natural or synthetic polyelectrolytes.

At low C and high LWE concentration, which corresponds to the dilute regime, we compared the effects of salt and acid addition on the interactions in solution. Repulsive electrostatic interactions decrease faster upon acid addition due to the associated shift of the acido-basic equilibrium that decreases the dissociation of the first carboxylic group in maleic acid copolymers.

In the remaining region of the $C–C_S$ diagram, the chains overlap due to high enough polymer concentration and/or chain expansion (low salt limit). The slow mode of relaxation that appears in the correlation functions is related to the presence of aggregates. The proposed driving force for the progressive aggregation is the lactonization of the monomers that decreases their solubility. As a consequence, the dynamical properties evolve with time and ultimately a phase separation occurs. This time evolution is faster for high polymer and salt concentrations, where the intermolecular aggregation is favored by the overlap of the chains and the repulsive electrostatic interactions are screened.

These results provide guidelines to define experimental conditions that will improve the time stability of the aqueous solutions of maleic acid–vinyl acetate copolymers. Furthermore they will help to discriminate in future work the self-association of the chains and the formation of intermacromolecular complexes, when other synthetic or natural polymers are present in solution, in particular in a biological context.

Acknowledgements

This work was performed during the stay of G.C.C. and M.S. in Strasbourg and G.C.C. is very grateful for the grant offered by the French Ministry of Foreign Affairs by means of CROUS Strasbourg.

References

[1] Breslow DS. Pure Appl Chem 1976;46:103.
[2] Maeda H. Adv Drug Delivery Rev 1991;6:181.
[3] Hirano T, Todoroki T, Kato S, Yamamoto H, Calicetti P, Veronese F, Maeda H, Ohashi S. J Control Release 1994;28:203 and subsequent papers.
[4] Hodnett EM, Wai Wu A, French FA. Eur J Med Chem 1978;13:577 and subsequent papers.
[5] Sato T, Kojime K, Ihda T, Sunamoto J, Ottenbrite RM. J Bioact Compatible Polym 1986;1:448 and subsequent papers.
[6] Nagasawa M, Rice SA. J Am Chem Soc 1960;82:5070.
[7] Bianchi E, Cifferi A, Parodi R, Rampone R, Tealdi A. J Phys Chem 1970;74:1050.
[8] Schultz AW, Strauss UP. J Phys Chem 1972;76:1767.
[9] Minakata A, Matsumura K, Sasaki S, Ohnuma H. Macromolecules 1980;13:1549.
[10] Kitano T, Kawaguchi S, Anazawa N, Minakata A. Macromolecules 1987;20:2498.
[11] Begala AJ, Strauss UP. J Phys Chem 1972;76:254.
[12] Delben F, Paoletti S. J Phys Chem 1974;78:1486.
[13] Kawaguchi S, Kitano T, Ito K, Minakata A. Macromolecules 1991;24:6335.
[14] Dubin PL, Strauss UP. J Phys Chem 1970;74:2482.
[15] Fenyo JC, Delben F, Paoletti S, Crescenzi V. J Phys Chem 1977;81:1900.
[16] Okuda T, Ohno N, Nitta K, Sugai S. J Polym Sci: Polym Phys Ed 1977;15:749.
[17] Ohno N, Sugai SJ. Macromol Sci Chem A 1990;27:861.
[18] Dubin PL, Strauss UP. J Phys Chem 1973;77:1427.
[19] Shimizu T, Minakata A, Tomiyama T. Polymer 1980;21:1427.
[20] Meullenet JP, Schmitt A, Candau SJ. Chem Phys Lett 1978;55:523.
[21] Xia J, Dubin PL, Kim Y, Muhoberac BB, Klimkowski VJ. J Phys Chem 1993;97:4528 and their subsequent papers.
[22] Katayose S, Kataoka K. Bioconjugate Chem 1997;8:702.
[23] Dash PR, Toncheva V, Schacht E, Seymour LW. J Control Release 1997;48(2-3):269.
[24] Carpov A, Chitanu GC, Maftei M, Zamfir A. Rom. Pat., 70120/1979; CA 95/1981, 187905 a.
[25] Methoden der organischen Chemie (Houben-Weyl). Erweiterungs- und Folgebaende zur vierten Auflage, Bd. E20, Makromolekulare Stoffe, hrsgb. Bartl, H. u. Falbe, J. Stuttgart: Georg Thieme Verlag, 1987.
[26] Riddick JA, Burger WA. Organic solvents, 3. New York: Wiley, 1970.
[27] Caze C, Decroix JC, Loucheux C, Nicco A. Bull Soc Chim Fr 1973;11:2977.
[28] Aida H, Urushizaki H, Takeuchi H. Fukui Daigaku Kogakubu Kenkyu Hokoku 1970;18:173.
[29] Caze C, Loucheux C. J Macromol Sci Chem A 1981;15:95.
[30] Aida H, Yoshida T, Matsuyama A. Fukui Daigaku Kogakubu Kenkyu Hokoku 1968;16:103; CA 71/1969, 102268b.
[31] Reed WF, Ghosh S, Medjahdi G, Francois J. Macromolecules 1991;24:6189.
[32] Provencher SW. Comput Phys Commun 1982;27:229.
[33] Minsk LM, Waugh LM, Kenyon OW. J Am Chem Soc 1950;72:2646.
[34] Dusek K, Klaban I, Kopecka J. Vysokomol Soedin 1962;4:1596.
[35] Chitanu GC, Carpov A, Asaftei T. Rom. Patent, 106745/1993.
[36] Nishio T, Minakata A. Rep Progr Polym Phys Jpn 1985;28:29.
[37] Mathiez P, Mouttet C, Weisbuch G. Biopolymers 1981;20:2381.
[38] Smits RG, Kuil ME, Mandel M. Macromolecules 1994;27:5599.
[39] Koene R, Mandel M. Macromolecules 1983;16:973.
[40] Koene R, Mandel M. Macromolecules 1983;16:220.
[41] Koene R, Mandel M. Macromolecules 1983;16:227.
[42] Sedlák M, Amis EJ. J Chem Phys 1992;96:817.
[43] Sedlák M, Amis EJ. J Chem Phys 1992;96:826.
[44] Chitanu GC, Zaharia IL, Carpov A. Int J Polym Anal Charact 1997;4:1 and Refs. [76,88,98,101,107] therein.
[45] Burchard W. Adv Pol Sci 1983;48:1.
[46] Zhou Z, Chu B, Peiffer DG. Macromolecules 1993;26:1876.
[47] Raspaud E, Lairez D, Adam M, Carton JP. Macromolecules 1994;27:2956.
[48] Zhang Y, Wu C, Fang Q, Zhang Y-X. Macromolecules 1996;29:2494.
[49] Sun T, King HE. Macromolecules 1996;29:3175.
[50] Klucker R, Munch JP, Schosseler F. Macromolecules 1997;30:3839.
[51] Joanny JF, Pincus P. Polymer 1980;21:274.
[52] Skouri R. Thèse Université Louis Pasteur, Strasbourg, 1994.
[53] Odijk T. Macromolecules 1979;12:688.
[54] Degiorgio V, Mantegazza F, Piazza R. Europhys Lett 1991;15:75.
[55] Barrat JL, Joanny JF. Europhys Lett 1993;24:333.
[56] Barrat JL, Joanny JF. J Phys II 1994;4:1089.
[57] Dobrynin AV, Colby RH, Rubinstein M. Macromolecules 1995;28:1859.
[58] Essafi W, Lafuma F, Williams CE. J Phys II 1995;5:1269.
[59] Sedlák M. J Chem Phys 1996;105:10 123 and references therein.